Spectral evidence for weathered basalt as an alternative to andesite in the northern lowlands of Mars

Michael B. Wyatt & Harry Y. McSween Jr

Department of Geological Sciences, University of Tennessee, Knoxville, Tennessee 37996, USA

Mineral abundances derived from the analysis of remotely sensed thermal emission data from Mars have been interpreted to indicate that the surface is composed of basalt (Surface Type 1) and andesite (Surface Type 2)[1]. The global distribution of these rock types is divided roughly along the planetary dichotomy which separates ancient, heavily cratered crust in the southern hemisphere (basalt) from younger lowland plains in the north (andesite)[1]. But the existence of such a large volume of andesite is difficult to reconcile with our present understanding of the geological evolution of Mars. Here we reinterpret martian surface rock lithologies using mineral abundances from previous work[1] and new mineralogies derived from a spectral end-member set representing minerals common in unaltered and low-temperature aqueously altered basalts. Our results continue to indicate the dominance of unaltered basalt in the southern highlands, but reveal that the northern lowlands can be interpreted as weathered basalt as an alternative to andesite. The coincidence between locations of such altered basalt and a suggested northern ocean basin implies that lowland plains material may be composed of basalts weathered under submarine conditions or weathered basaltic sediments transported into this depocentre.

The identification of basalt on Mars from Thermal Emission Spectrometer (TES) observations[1,2] agrees with visible/near-infrared spectroscopic observations of low-albedo regions[3]. The identification of andesite on Mars from TES observations[1] is consistent with chemical analyses of rocks by the Mars Pathfinder[4]. Additional calibrations using a variety of unweathered terrestrial volcanic rocks have demonstrated the fidelity with which thermal emission data can distinguish basalt and andesite[5], and these results[6] support the identification of basaltic and andesitic martian surface compositions.

The large expanse of andesite in the northern plains as suggested by Bandfield *et al.*[1] is, however, difficult to explain. On Earth, andesite forms mostly at subduction zones, where water released from descending slabs promotes mantle melting. However, there is no evidence for subduction on Mars. Although andesite can also be produced during fractionation of basaltic magma, this process is inefficient and could not account for a large volume of andesite[7]. Less fractionation is required for hydrous basaltic melts to reach the composition of andesite, and evidence exists that some martian basaltic meteorites contained water[8]. In this case, however, the northern plains should consist of comparable amounts of andesite and basalt.

The observed geographic concentration of martian andesite within the northern lowlands[1] suggests an alternative mechanism for their formation. Previous abstracts have indicated that weathered or oxidized basaltic glass is spectrally similar to andesitic glass[9,10]. Here, we explore whether Surface Type 2 (andesite) might be reinterpreted as basalt weathered in a submarine environment. The northern lowlands lie, for the most part, below the 0-km elevation datum, and lakes or oceans, possibly fed by large outflow channels originating in the southern highlands, may have occupied this region[11]. Deconvolved mineral abundances from ref. 1 and new mineralogies derived from TES data and terrestrial basalts using a

spectral end-member set representing minerals common in unaltered and low-temperature aqueously altered basalts are used to reclassify martian surface lithologies.

Figure 1a and b compare spectral fits and modelled mineral abundances produced by linear deconvolutions of Surface Types 1 and 2 spectra (see Methods). Bandfield *et al.*[1] used 45 spectral end-members[12] representing igneous, sedimentary and metamorphic minerals, whereas Hamilton *et al.*[6] used a narrower range of 29 mineral spectra representing mostly unweathered basalts and andesites. Our 39 spectral end-members represent minerals common in unaltered and low-temperature aqueously altered basalts[13] (Table 1 of the Supplementary Information). One of the primary differences between the spectral end-member sets of refs 1 and 6 and the end-member set used here is the omission of a high-silica glass phase[5] in
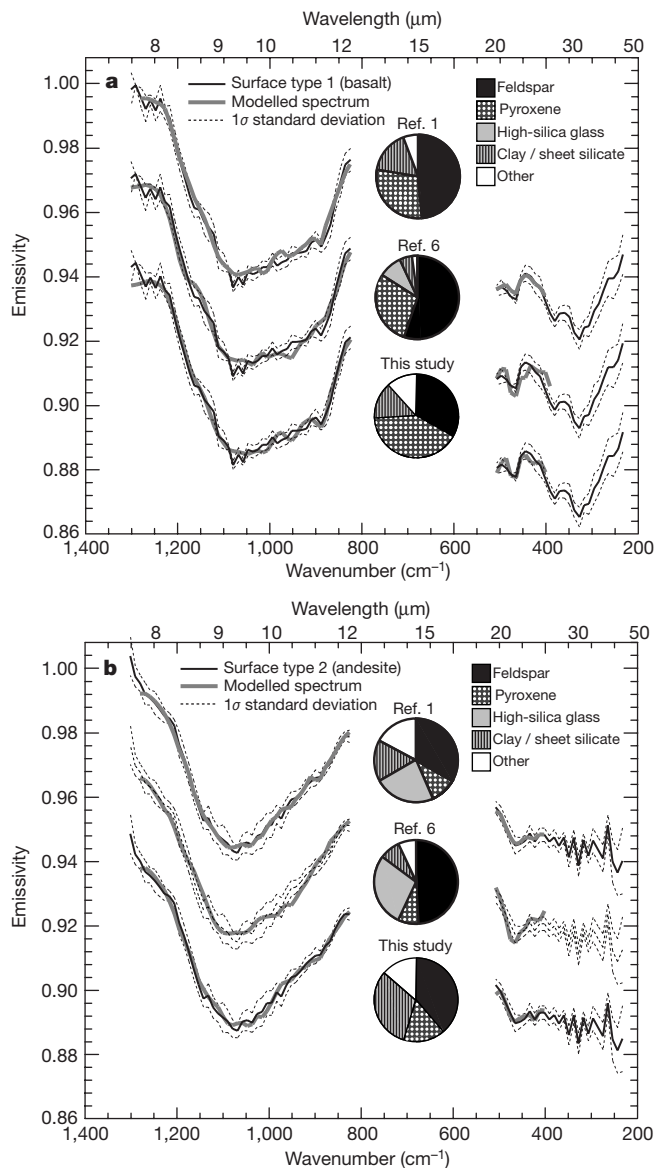
Figure 1 Comparison of martian surface spectra and modelled spectral fits. **a**, **b**, Martian Surface Type 1 (**a**) and Type 2 (**b**) spectra and modelled spectral fits (offset by 0.028 emissivity for clarity) and mineral abundances produced by linear deconvolution from Bandfield *et al.*[1], Hamilton *et al.*[6] and this study (Table 2 of the Supplementary Information). The detection limit for mineral abundances deconvolved from TES spectra is 10–15 vol.% (ref. 2). Mineral abundances for Surface Type 2 are characteristic of either andesitic or weathered basaltic compositions.

this study (see Methods). A similar difference involving K-feldspar occurs between the end-member set used by ref. 6 compared to those used by ref. 1 and this study (see Methods). Also shown in Fig. 1a and b are 1σ standard deviations for martian surface spectra as determined by ref. 1.

Spectral fits produced by linear deconvolution of the Surface Type 1 spectrum show low root-mean-square (r.m.s.) values of 0.0018 (ref. 1), 0.0026 (ref. 6), and 0.0018 (this study). Modelled mineral abundances for the three end-member sets (Fig. 1a, Table 2 of the Supplementary Information) are all characterized by high values of plagioclase and pyroxene, and low values of weathering products (clays, sulphates and carbonates). The low r.m.s. values and similar modelled mineral abundances derived from different end-member sets indicate these modes accurately reflect the Surface Type 1 composition. The modelled mineral abundances, and the broad, slightly squared shape absorption between ~800–1,200 cm^{-1} characteristic of Surface Type 1, are representative of unweathered

Figure 2 Spectral comparisons of glass, clays, terrestrial basalt and martian surface spectra. **a**, **b**, High-silica glass and two clays (Fe-smectite and Ca-montmorillonite) (**a**) and fresh-cut and weathered surface of a CRB sample[5,6] (**b**) compared to Surface Type 1 and 2 spectra, respectively (offset by 0.06 emissivity for clarity). Blackbody was added to each terrestrial rock sample to account for band-depth particle-size effects.

basaltic compositions[1,2,5,6].

Analogous spectral fits of the Surface Type 2 spectrum show low r.m.s. values of 0.0009 (ref. 1), 0.0023 (ref. 6), and 0.0014 (this study). However, modelled mineral abundances differ, resulting in an ambiguous description of the Surface Type 2 composition (Fig. 1b, Table 2 of the Supplementary Information). The results of refs 1 and 6 are characterized by high modelled abundances of plagioclase and high-silica glass and low abundances of pyroxene and weathering products. Modelled abundances in this study are characterized by plagioclase with appreciable alteration minerals (clays and K-feldspar) and lesser pyroxene. The well-modelled spectra indicate that each of the different mineral modes is equally valid for describing the Surface Type 2 spectrum. Modelled mineral abundances from refs 1 and 6, and the slightly V-shaped absorption between ~800–1,200 cm^{-1} characteristic of Surface Type 2, are representative of andesite[1,5,6]. Higher abundances of clays and K-feldspar, and lower abundances of pyroxenes for Surface Type 2 as modelled in this study, are characteristic of altered basalt[13].

Modelled mineral abundances supporting a weathered basalt composition are largely a result of clays replacing high-silica glass. Absorption features between 500–550 cm^{-1} in laboratory spectra distinguish clays modelled in this study (Fe-smectite and Ca-montmorillonite) from high-silica glass (Fig. 2a); however, the CO_2 atmosphere of Mars is largely opaque in this spectral region, which limits its usefulness for analysis of surface compositions. The spectral regions of high-silica glass and clays used for analysis of martian surface compositions are very similar in their overall spectral shape and positions of spectral features. Future work is needed to understand better the degree of substitution and spectral effects of varying crystallinity in amorphous phases over a range of chemical compositions. Despite this ambiguity, conclusions from deconvolved TES spectra concerning other rock-forming minerals are thought to be robust[1,2,5,6].

Figure 2b shows spectra of the fresh-cut and weathered surfaces of a Columbia River Flood Basalt (CRB sample 4, refs 5, 6) re-sampled to TES spectral resolution compared to Surface Type 1 and 2 spectra, respectively. Because martian surface spectra analysed by TES are thought to be dominated by sand-sized particles[12,1] rather than bedrock, a blackbody component (which does not affect spectral shape) was added to each terrestrial sample to account for band-depth particle-size effects. The spectrum of the fresh-cut CRB surface displays a broad, slightly squared shape absorption between ~800–1,200 cm^{-1} similar to the Surface Type 1 spectrum, whereas the spectrum of the natural CRB surface displays a more V-shaped absorption similar to the Surface Type 2 spectrum. Spectral fits produced by linear deconvolution of the fresh-cut CRB surface spectrum show low r.m.s. values (0.0020 (ref. 1), 0.0025 (ref. 6), 0.0031 (this study)), and deconvolved mineral abundances are characterized by high values of plagioclase and pyroxene, and low values of weathering products (Table 3 of the Supplementary Information), similar to Surface Type 1. Spectral fits produced by linear deconvolution of the natural CRB surface spectrum show analogous low r.m.s. values (0.0023 (ref. 1), 0.0034 (ref. 6), 0.0030 (this study)). However, modelled mineral abundances for the natural CRB surface using the end-member sets of Bandfield et al.[1] and Hamilton et al.[6] are characterized by high abundances of plagioclase, pyroxene and high-silica glass, whereas abundances in this study are characterized by plagioclase with appreciable alteration minerals and lesser pyroxene (Table 3 of the Supplementary Information), similar to the ambiguous mineralogic characterization of Surface Type 2.

Microscopic examination of the fresh-cut and natural CRB surfaces agrees best with deconvolved mineral abundances from Bandfield et al.[1] in which a combination of plagioclase, pyroxene, high-silica glass and clays comprises the sample's modal mineralogy. A decrease in pyroxene and increase in clay abundances is expected on a natural surface as pyroxenes are typically weathered to clays.

However, an increase in the abundance of high-silica volcanic glass on a natural surface is not expected, because such a phase is also easily weathered. The increase in modelled high-silica glass from the fresh-cut to the natural CRB surface might indicate the formation of amorphous silica alteration products which are spectrally similar to high-silica glass. The original interpretation of the high-silica glass spectral end-member phase as a primary volcanic glass may be too limited, as it could also represent an amorphous high-silica alteration product.

Figure 3 compares the global distribution of Surface Types 1 and 2, as determined in ref. 1 and global topography determined from Mars Orbiter Laser Altimeter (MOLA) data[14] in hemispherical north and south stereographic polar projections. The highest concentrations of Surface Type 1 (green) in the southern highlands and Surface Type 2 (red) in the northern lowlands coincide roughly with the planetary dichotomy, although there is some mixing of surface types across this divide. Blue pixels on TES composition maps represent regions covered by fine-grained bright dust which blankets the surface and prohibits spectral analysis of sand and rock compositions. Also shown on the north polar projections is a white line defining contacts previously interpreted as shorelines[15] which approximate an equipotential line[11]. Surface Type 2 compositions in the northern hemisphere are distributed almost entirely within the proposed shorelines where they are not spectrally obscured by dust cover. Surface Type 2 compositions in the southern hemisphere may be due to similar alteration processes, but the lack of geographic

concentrations does not support a large southern hemisphere body of water.

Linear deconvolution of the Surface Type 2 spectrum by ref. 1 and this study requires some clay/sheet silicates to be modelled at or above the TES detectability limit[2]. The high abundance of modelled alteration products in this study results from the spectral similarities and substitution of clays for high-silica glass at TES spectral resolution. High abundances of well crystalline phyllosilicates in low-albedo regions are not supported by Phobos Infrared Spectrometer (ISM) data[16]; however, poorly crystalline palagonite has been proposed as a component in bright martian soil[17]. We note that ISM data only covered ~20% of the martian equatorial region, which is dominated by unweathered basaltic compositions as determined by TES data. Comparison of ISM data with weathered basalt compositions in the northern hemisphere is thus not possible. Merényi et al.[18] did observe northern regions from high-spectral-resolution telescopic images and noted that weaker mafic mineral bands could be explained by a higher glass content. This is generally analogous to the increased glass content determined[1] (interpreted here as a possible alteration product) to explain differences in the Surface Type 1 and 2 spectra. The mineralogies determined by Bandfield et al.[1] and this study for Surface Type 2 can thus both be interpreted as representing weathered basalt.

A martian crust dominated by basalt containing augite and pigeonite (Table 3 of the Supplementary Information) is in agreement with visible/near-infrared spectroscopic observations of low-
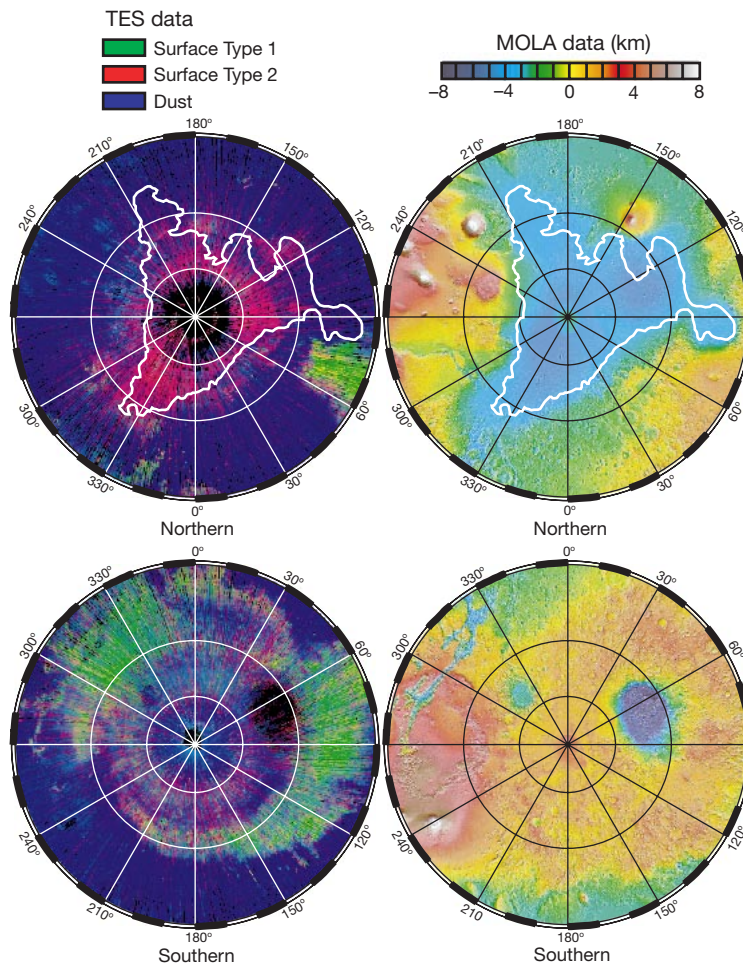
Figure 3 Global distribution of Surface Types 1 and 2 as determined by ref. 1 and global topography determined from MOLA data[14]. Surface Type 2 compositions in the northern

hemisphere map closely to a proposed ocean basin[11], as delineated by elevation and a possible shoreline (white line)[15].

albedo regions that suggest surface materials may be similar to shergottite meteorites[3]. Analysis of depressions ("ghost craters") in the lowlands indicate that the basement there is of Noachian age[19], like the southern highlands, so it is plausible that the entire planet had an ancient basaltic crust that was altered where water ponded. This hypothesis may also explain the absence of andesite among martian meteorites, because either this material might exist only as weathering rinds or more thoroughly weathered rocks might not survive impact ejection. McSween and Keil[20] compared compositions of martian soils and concluded that the global dust formed by weathering of basalts rather than andesites. Although the existence of andesite on Mars remains a viable hypothesis, linear deconvolution of martian thermal infrared spectra, spectral matching with terrestrial volcanic rocks, and the geographic distribution of the Surface Type 2 spectrum suggest that martian northern lowland plains materials are basalts weathered under submarine conditions and/or sediments derived from weathered basalt and deposited in this basin. □

Methods

Linear deconvolutions using three spectral end-member sets[12] (refs 1, 6 and this study) were run for each martian surface spectrum. Algorithm outputs include a best-fit model spectrum for each martian surface spectrum, percentage of each mineral end-member used, and an r.m.s. error value (average error over the entire spectrum). The r.m.s. value indicates goodness of fit for a particular model iteration for the same martian spectrum, rather than a comparison between fits of the two martian spectra. Spectral fitting for both methods was constrained to $1,280-400$ cm^{-1}, although TES data cover the wavenumber range of $1650-200$ cm^{-1}. The atmospheric correction used to derive the TES surface spectra used in this study did not include the high wavenumber range of TES data owing to numerous water vapour and minor CO_2 features. Furthermore, there are no fundamental silicate features in the $1,650-1,400$ cm^{-1} region. Similar to ref. 1 the deconvolution algorithm also did not use the $400-200$ cm^{-1} spectral range. Residual atmospheric water vapour rotational bands are apparent in both the martian surface spectra as well as in the Arizona State University (ASU) mineral library end-member spectra. This restricted wavenumber range prevents the deconvolution algorithm from attempting to fit water vapour features instead of surface mineralogy.

Accurate deconvolution is largely dependent on spectral end-member sets representing an appropriate range of compositions in the mixture. The high-silica glass phase (77.9% SiO_2, 12.6% Al_2O_3, 3.90% Na_2O, 5.67% K_2O) not included in the end-member set used in this study has been interpreted[1,5,6] as representing a primary volcanic glass. High-silica volcanic glasses are often not present in high abundances in unweathered basalts, compared to andesites, and typically alter to clays in a weathering environment. For these reasons, we have excluded this volcanic glass phase in our end-member set that is designed to represent basalts and low-temperature aqueously altered basalts. K-feldspar is not included in the Hamilton et al.[6] spectral end-member set as it is not typically found in unweathered basalt and andesite. K-feldspar is however included by Bandfield et al.[1] to represent possible mineralogies in a larger suite of igneous, metamorphic and sedimentary rock types and in this study as a possible alteration product[13].

1. Bandfield, J. L., Hamilton, V. E. & Christensen, P. R. A global view of martian surface compositions from MGS-TES. *Science* **287**, 1626–1630 (2000).
2. Christensen, P. R. *et al.* Identification of a basaltic component on the martian surface from Thermal Emission Spectrometer data. *J. Geophys. Res.* **105**, 9609–9621 (2000).
3. Mustard, J. F., Murchie, S., Erard, S. & Sunshine, J. M. In situ compositions of martian volcanics: Implications for the mantle. *J. Geophys. Res.* **102**, 25605–25615 (1997).
4. Rieder, R. *et al.* The chemical composition of martian soils and rocks returned by the mobile alpha proton X-ray spectrometer: Preliminary results from the X-ray mode. *Science* **278**, 1771–1774 (1997).
5. Wyatt, M. B. *et al.* Analysis of terrestrial and martian volcanic compositions using thermal emission spectroscopy: I. Determination of mineralogy, chemistry, and classification strategies. *J. Geophys. Res.* **106**, 14711–14732 (2001).
6. Hamilton, V. E. *et al.* Analysis of terrestrial and martian volcanic compositions using thermal emission spectroscopy: II. Application to martian surface spectra from the Mars Global Surveyor Thermal Emission Spectrometer. *J. Geophys. Res.* **106**, 14733–14746 (2001).
7. McSween, H. Y. Jr *et al.* Chemical, multispectral, and textural constraints on the composition and origin of rocks at the Mars Pathfinder landing site. *J. Geophys. Res.* **104**, 8679–8715 (1999).
8. McSween, H. Y. Jr *et al.* Geochemical evidence for magmatic water within Mars from pyroxenes in the Shergotty meteorite. *Nature* **409**, 487–490 (2001).
9. Noble, S. K. & Pieters, C. M. Type 2 terraine: compositional constraints on the martian lowlands. *Lunar Planet. Sci. Conf.* **XXXII**, [online] CD 1230 (2001).
10. Minitti, M. E., Rutherford, M. J. & Mustard, J. F. The effects of oxidation on spectra of SNC-like basalts: Application to Mars remote sensing. *Lunar Planet. Sci. Conf.* **XXXI**, [online] CD 1282 (2000).
11. Head, J. W. *et al.* Possible ancient oceans on Mars; evidence from Mars Orbiter laser altimeter data. *Science* **286**, 2134–2137 (1999).
12. Christensen, P. R. *et al.* A thermal emission spectral library of rock forming minerals. *J. Geophys. Res.* **105**, 9735–9739 (2000).
13. Thompson, G. in *Hydrothermal Processes at Seafloor Spreading Centers* (eds Rona, P. A., Bostrom, K., Laubier, L. & Smith, K. L. Jr) 225–278 (Plenum, New York, 1983).
14. Smith, D. E. *et al.* The global topography of Mars and implications for surface evolution. *Science* **284**, 1495–1503 (1999).
15. Parker, T. J. *et al.* Transitional morphology in the west Deuteronilus Mensae region of Mars: implications for modification of the lowland/upland boundary. *Icarus* **82**, 111–145 (1989).
16. Murchie, S., Kirkland, L., Erard, S., Mustard, J. & Robinson, M. Near-infrared spectral variations of martian surface materials from ISM imaging spectrometer data. *Icarus* **147**, 444–471 (2000).
17. Murchie, S. *et al.* Spatial variations in the spectral properties of bright regions on Mars. *Icarus* **105**, 454–468 (1993).
18. Merényi, E., Singer, R. B. & Miller, J. S. Mapping of spectral variations on the surface of Mars from high spectral resolution telescopic images. *Icarus* **124**, 280–295 (1996).
19. Frey, H. V. *et al.* A very large population of likely buried impact basins in the northern lowlands of Mars revealed by MOLA data. *Lunar Planet. Sci. Conf.* **XXXII**, [on line] CD 1680 (2001).
20. McSween, H. Y. Jr & Keil, K. Mixing relationships in the martian regolith and the composition of globally homogenous dust. *Geochim. Cosmochim. Acta* **64**, 2155–2166 (2000).

....

Formation of tough interlocking microstructures in silicon nitride ceramics by dynamic ripening

Zhijian Shen, Zhe Zhao, Hong Peng & Mats Nygren

Department of Inorganic Chemistry, BRIIE Center for Inorganic Interfacial Engineering, Arrhenius Laboratory, Stockholm University, S-106 91 Stockholm, Sweden

....

Ceramics based on Si_3N_4 have been comprehensively studied and are widely used in structural applications[1,2]. The development of an interlocking microstructure of elongated grains is vital to ensure that this family of ceramics have good damage tolerance[3,4]. Until now this has been accomplished by heating the appropriate powder compacts to temperatures above $1,700\,°C$ for extended periods. This procedure involves a necessary step of controlling the size and population of seeds—added *ex situ* or formed *in situ*—to ensure selective grain growth[5,6]. Here we report the very fast (within minutes) *in situ* formation of a tough interlocking microstructure in Si_3N_4-based ceramics. The microstructures are obtained by a dynamic ripening mechanism, an anisotropic Ostwald ripening process that results from the rapid heating rate. The resulting microstructures are uniform and reproducible in terms of grain size distribution and mechanical properties, and are easily tailored by manipulating the kinetics. This process is very efficient and opens up new possibilities to optimize mechanical properties and cost-effectively manufacture ceramics.

Sintering Si_3N_4-based ceramics is a complex process, during which densification, phase transformation and grain growth take place simultaneously. Therefore, it is not an easy task to clarify the mechanisms determining the rate of grain growth, for example. Research carried out during recent years indicates that the grain growth is dominated by an Ostwald ripening mechanism driven by the reduction of interface energy, that is, the smallest grains deriving from the precursor powder and early precipitates dissolve in the